

Molecular Determinants of Proteolytic Disassembly of the Reovirus Outer Capsid*

Received for publication, December 16, 2011, and in revised form, January 16, 2012. Published, JBC Papers in Press, January 17, 2012, DOI 10.1074/jbc.M111.334854

Joshua D. Doyle^{‡§}, Pranav Danthi^{§¶1}, Emily A. Kendall^{§¶2}, Laura S. Ooms^{‡§}, J. Denise Wetzel^{§¶}, and Terence S. Dermody^{‡§¶3}

From the Departments of [‡]Pathology, Microbiology, and Immunology and [¶]Pediatrics and the [§]Elizabeth B. Lamb Center for Pediatric Research, Vanderbilt University School of Medicine, Nashville, Tennessee 37232

Background: The reovirus outer capsid protein $\sigma 3$ acts as a substrate for intracellular proteases.

Results: Two polymorphic amino acids in $\sigma 3$ act in opposition to determine protease sensitivity, disassembly kinetics, and biochemical stability.

Conclusion: A regulatory network of residues maintains optimal reovirus outer capsid function.

Significance: The balance between stability and instability of capsid structures is likely to be an important determinant of viral fitness.

Following attachment and internalization, mammalian reoviruses undergo intracellular proteolytic disassembly followed by viral penetration into the cytoplasm. The initiating event in reovirus disassembly is the cathepsin-mediated proteolytic degradation of viral outer capsid protein $\sigma 3$. A single tyrosine-to-histidine mutation at amino acid 354 (Y354H) of strain type 3 Dearing (T3D) $\sigma 3$ enhances reovirus disassembly and confers resistance to protease inhibitors such as E64. The $\sigma 3$ amino acid sequence of strain type 3 Abney (T3A) differs from that of T3D at eight positions including Y354H. However, T3A displays disassembly kinetics and protease sensitivity comparable with T3D. We hypothesize that one or more additional $\sigma 3$ polymorphisms suppress the Y354H phenotype and restore T3D disassembly characteristics. To test this hypothesis, we engineered a panel of reovirus variants with T3A $\sigma 3$ polymorphisms introduced individually into T3D- $\sigma 3$ Y354H. We evaluated E64 resistance and *in vitro* cathepsin L susceptibility of these viruses and found that one containing a glycine-to-glutamate substitution at position 198 (G198E) displayed disassembly kinetics and E64 sensitivity similar to those properties of T3A and T3D. Additionally, viruses containing changes at positions 233 and 347 (S233L and I347T) developed *de novo* compensatory mutations at position 198, strengthening the conclusion that residue 198 is a key determinant of $\sigma 3$ proteolytic susceptibility. Variants with Y354H in $\sigma 3$ lost infectivity more rapidly than T3A or T3D following heat treatment, an effect abrogated by G198E. These results identify a regulatory network of residues that control $\sigma 3$ cleavage and capsid stability, thus providing insight into the regulation of nonenveloped virus disassembly.

All viruses must transit host cell membranes, either at the cell surface or following particle internalization, to productively infect cells. Enveloped viruses, such as orthomyxoviruses (1, 2), paramyxoviruses (3), and retroviruses (4, 5), encode proteins that mediate fusion of the viral envelope with target cell membranes, thus facilitating viral cell entry. Nonenveloped viruses, such as adenovirus (6) and reovirus (7), traverse cellular membranes despite the absence of a viral envelope. The capsid proteins of nonenveloped viruses often contain hydrophobic motifs that are exposed in response to receptor binding or endosomal cues. These motifs in turn disrupt host cell membranes and mediate viral access to the cytosol. The viral machinery that guides the virus into the cell interior must be tightly regulated to ensure its activation only at the appropriate time and in the correct compartment to ensure productive infection.

Mammalian orthoreoviruses (reoviruses) are nonenveloped, icosahedral viruses that contain a double-stranded RNA genome housed within two concentric protein shells, an outer capsid, composed primarily of viral proteins $\sigma 3$ and $\mu 1$, and an inner core (8, 9). Following binding to cell-surface receptors, including sialylated glycans and junctional adhesional molecule-A (JAM-A), reovirus particles are internalized via $\beta 1$ integrin-dependent, clathrin-mediated endocytosis (10–13). Internalized viral particles undergo a stepwise disassembly process. The initial event in reovirus disassembly is the proteolytic cleavage of $\sigma 3$ protein, which is catalyzed by endosomal cathepsin proteases (14–16). Ablation of cathepsin activity by either pharmacological (7, 14) or genetic (16) means abolishes reovirus infectivity, suggesting that $\sigma 3$ cleavage is essential for reovirus disassembly and productive infection. Proteolytic removal of $\sigma 3$ facilitates cleavage of $\mu 1$ to generate the fragments δ and φ , resulting in formation of infectious subviral particles (7, 17, 18). Infectious subviral particles feature exposed membrane interaction motifs and transit across membranes, leading to the delivery of viral core particles into the cytosol (19). Infectious subviral particles can be generated *in vitro* using several proteases, including cathepsins B and L (7, 16, 20).

* This work was supported, in whole or in part, by National Institutes of Health Grants T32 GM008554 from USPHS (to J. D. D.) and R01 AI032539 (to T. S. D.). This work was also supported by the Elizabeth B. Lamb Center for Pediatric Research.

¹ Present address: Dept. of Biology, Indiana University, Bloomington, IN 47405.

² Present address: Dept. of Medicine, Massachusetts General Hospital, Boston, MA 02114.

³ To whom correspondence should be addressed: Lamb Center for Pediatric Research, D7235 MCN, Vanderbilt University School of Medicine, Nashville, TN 37232. Tel.: 615-343-9943; Fax: 615-343-9723; E-mail: terry.dermody@vanderbilt.edu.

Determinants of Reovirus Outer Capsid Disassembly

Structural determinants of $\sigma 3$ cathepsin-cleavage susceptibility are not well defined. Putative cathepsin L cleavage sites between residues 243–244 and 250–251 have been identified in reovirus strain type 1 Lang (T1L)⁴ $\sigma 3$ (16), and this region is conserved between T1L and strain type 3 Dearing (T3D). However, structural models of $\sigma 3$ (21) indicate that these cleavage sites are masked by the $\sigma 3$ carboxyl-terminal domain (C terminus). Additional evidence suggests that the C terminus determines $\sigma 3$ protease susceptibility (22). Mutant viruses isolated from persistently infected cultures have increased protease susceptibility (23), a phenotype that genetically segregates with a tyrosine-to-histidine mutation at amino acid position 354 (Y354H) in $\sigma 3$ (22), which is located in the C terminus of the protein. The Y354H mutation increases the rate at which $\sigma 3$ is cleaved by proteases *in vitro* and confers resistance to protease inhibitors, such as the pan-cysteine protease inhibitor E64 and ammonium chloride, which inhibits vacuolar acidification (14, 22, 24). The mechanism by which Y354H enhances the protease sensitivity of $\sigma 3$ is unclear, but it is possible that His-354 alters the intramolecular localization of the C terminus and exposes the normally occluded protease cleavage sites (22).

The relationship between the stability of nonenveloped virus capsid structures and viral fitness is poorly defined. Mutations that enhance outer capsid proteolysis, such as Y354H, accelerate the kinetics of viral entry into tissue culture cells and enable viral replication in settings of diminished protease availability. However, this mutation is absent from most primary reovirus isolates (25), suggesting that it imposes a fitness penalty on the virus. Interestingly, the deduced $\sigma 3$ amino acid sequence of strain type 3 Abney (T3A) (26) contains a native histidine at residue 354 (25). Determining how His-354 in T3A $\sigma 3$ affects cell entry, viral disassembly, and viral replication should provide information about how nonenveloped viruses maintain the optimum balance between capsid stability and instability and further an understanding of the fitness implications of perturbing that balance.

In this study, we compared disassembly kinetics and sensitivity to protease inhibitors of T3A and T3D. The deduced $\sigma 3$ amino acid sequence of T3D contains a tyrosine at residue 354, and there are seven additional amino acid polymorphisms between T3A and T3D $\sigma 3$ sequence. We engineered a panel of reovirus variants containing each of these native $\sigma 3$ polymorphisms in the context of $\sigma 3$ -Y354H to identify residues in $\sigma 3$ that modulate protease sensitivity. The panel of variants was tested for growth inhibition by E64 and disassembly mediated by cathepsin L *in vitro*. We identified a glycine-to-aspartate polymorphism at position 198 in $\sigma 3$ that is capable of independently suppressing the Y354H phenotype. We propose that residues 198 and 354 act in concert to maintain optimum stability of the reovirus capsid.

EXPERIMENTAL PROCEDURES

Cells and Viruses—Spinner-adapted murine L929 cells were grown in either suspension or monolayer cultures in Joklik's

spinner-modified Eagle's minimal essential medium (SMEM; Lonza, Walkersville, MD) supplemented to contain 5% fetal bovine serum (Invitrogen), 2 mM L-glutamine (Invitrogen), 100 units of penicillin/ml, 100 units of streptomycin/ml (Invitrogen), and 0.25 μ g of amphotericin/ml (Sigma-Aldrich). BHK-T7 (baby hamster kidney-T7) cells were grown in Dulbecco's modified Eagle's minimal essential medium (Invitrogen) supplemented to contain 5% fetal calf serum, 2 mM L-glutamine, 2% minimal essential medium amino acid solution (Invitrogen), and 1 mg of Geneticin/ml (Invitrogen).

Reovirus strain T3A is maintained as a laboratory stock. Recombinant strain (rs) T3D is a stock generated by plasmid-based reverse genetics from cloned T3D cDNAs (27). The engineered reovirus mutant rsT3D- $\sigma 3$ Y354H was generated as described (28).

Generation of Reovirus Variants—Viruses containing engineered changes in $\sigma 3$ protein were generated using reverse genetics (27). The S4 gene was excised from the pT7-M2-S2-S3-S4T3D plasmid (27) using HindIII and NheI to generate the tricistronic plasmid pT7-M2-S2-S3T3D. The pT7-S4T3D plasmid was used as template to generate pT7-S4T3DA28T+Y354H, pT7-S4T3DE108A+Y354H, pT7-S4T3DI180V+Y354H, pT7-S4T3DG198E+Y354H, pT7-S4T3DS215D+Y354H, pT7-S4T3DS233L+Y354H, and pT7-S4T3DI347T+Y354H using QuikChange mutagenesis (Stratagene, La Jolla, CA). Monolayers of BHK-T7 cells (27) at 90% confluency ($\sim 3 \times 10^6$ cells) seeded in 60-mm dishes (Costar; Corning Inc., Corning, NY) were co-transfected with 3.5 μ g each of five plasmids representing the cloned reovirus T3D genome using 3 μ l of TransIT-LT1 transfection reagent (Mirus Bio LLC; Madison, WI) per μ g of plasmid DNA. Following 72 h of incubation, recombinant virus was isolated from transfected cells by plaque purification using monolayers of L929 cells (29). Virus stocks were passaged, and titers were determined as described (30).

Growth of Virus in Cells Treated with E64—Confluent monolayers of L929 cells ($\sim 2 \times 10^5$ cells/well) in 24-well plates (Costar) were preincubated in SMEM supplemented to contain 0–200 μ M E64 (Sigma-Aldrich) at 37 °C for 4 h. The medium was removed, and cells were adsorbed with second- or third-passage virus stocks at an m.o.i. of 2 pfu/cell. After incubation at 4 °C for 1 h, the inoculum was removed, cells were washed with PBS, and 1 ml of fresh SMEM supplemented to contain 0–200 μ M E64 was added. Cells were incubated at 37 °C for 24 h and frozen and thawed twice. Viral titer in cell lysates was determined by plaque assay (29).

Treatment of Reovirus Virions with Cathepsin L—Purified reovirus virions at a concentration of 2×10^{12} particles/ml in reaction buffer L (100 mM NaCl, 15 mM MgCl₂, 50 mM sodium acetate (pH 5.0)) were treated with 50 μ g of purified, recombinant human cathepsin L (7) per ml in the presence of 5 mM dithiothreitol at 37 °C for 0–4 h. Aliquots were removed at various intervals, mixed with SDS sample buffer supplemented to contain 500 μ M E64, and incubated on ice for 5 min to terminate protease activity. Reaction mixtures were analyzed by SDS-PAGE.

SDS-PAGE of Reovirus Structural Proteins—Discontinuous SDS-PAGE was performed as described (31). Samples were incubated at 98 °C for 5 min, loaded into wells of precast 4–20%

⁴ The abbreviations used are: T1L, type 1 Lang; T3A, type 3 Abney; T3D, type 3 Dearing; SMEM, spinner-modified Eagle's minimal essential medium; Tricine, N-[2-hydroxy-1,1-bis(hydroxymethyl)ethyl]glycine; m.o.i., multiplicity of infection; rs, recombinant strain.

gradient Tris-Tricine polyacrylamide gels (Bio-Rad Laboratories), and electrophoresed at a constant voltage of 180 V for 1 h. Following electrophoresis, gels were stained using a Novex colloidal blue staining kit (Invitrogen) according to the manufacturer's instructions.

Densitometric Analysis of Reovirus Structural Proteins—Stained gels were visualized using an infrared imaging system (LI-COR Biosciences, Lincoln, NE). Band intensities in the scanned images were quantified using Odyssey Application software version 3.0.16 (LI-COR). The relative amount of $\sigma 3$ protein was determined by comparing the intensity of bands corresponding to $\sigma 3$, which has an apparent molecular mass of ~ 41 kDa, with bands corresponding to viral core protein $\sigma 2$, which has an apparent molecular mass of ~ 47 kDa and is not affected by protease treatment under these conditions (14).

Heat Resistance of Reovirus Virions—Purified reovirus virions at a concentration of 2×10^8 particles/ml in virion storage buffer (150 mM NaCl, 15 mM MgCl₂, 10 mM Tris (pH 7.4)) were treated at 55 °C for 60 min. At 15-min intervals, samples were removed and placed on ice. Viral titers were determined by plaque assay (28).

Specific Infectivity of Reovirus Virions—Fresh preparations of reovirus virions were generated in triplicate from second-passage lysate stocks as described (27). Particle density of each viral preparation was determined by quantifying absorbance at 260 nm and calculated using the equivalence of $1 A_{260} = 2.1 \times 10^{12}$ particles/ml (32). Titer of each preparation was determined by plaque assay (28).

Kinetic Ammonium Chloride Protection Assay—Confluent monolayers of L929 cells ($\sim 2 \times 10^5$ cells/well) in 24-well plates were adsorbed with second- or third-passage virus stocks at an m.o.i. of 25 pfu/cell. After incubation at 4 °C for 1 h, the inoculum was removed, cells were washed with PBS at 4 °C, and 1 ml of prewarmed SMEM was added. At various times after adsorption, 25 μ l of 1 M NH₄Cl was added to the medium to give a final concentration of 25 mM. At 20 h after adsorption, the medium was removed, and cell monolayers were fixed with 1 ml of methanol at -20 °C for a minimum of 30 min. Fixed monolayers were washed twice with PBS, blocked with 5% immunoglobulin-free BSA (Sigma-Aldrich) in PBS, and incubated at 37 °C for 30 min with rabbit polyclonal anti-reovirus serum at a 1:1000 dilution in PBS plus 0.5% Triton X-100. Monolayers were washed twice with PBS and incubated at 37 °C for 30 min with a 1:1000 dilution of anti-rabbit goat immunoglobulin conjugated with Alexa Fluor 488 (Molecular Probes, Inc., Eugene, OR). Monolayers were washed twice and visualized by indirect immunofluorescence. Reovirus antigen-positive cells were quantitated by enumerating fluorescent cells in three random fields of view per well at 100–400 \times magnification. Total cell number was quantified by enumerating 4',6-diamidino-2-phenylindole (DAPI)-stained nuclei.

RESULTS

T3A and T3D Are Sensitive to Protease Inhibitor E64—The deduced amino acid sequences of T3A and T3D $\sigma 3$ proteins contain eight polymorphic residues (Table 1). Several of the T3A-T3D polymorphic residues including 354 are found in the virion-distal region of $\sigma 3$, which is predicted to be accessible to

TABLE 1

Polymorphic residues between T3A and T3D $\sigma 3$

T3A and T3D differ at the eight indicated positions in the $\sigma 3$ open reading frame.

Virus strain	Amino acid position							
	28	108	180	198	215	233	347	354
T3A	Thr	Ala	Val	Glu	Asn	Leu	Thr	His
T3D	Ala	Glu	Ile	Gly	Ser	Ser	Ile	Tyr

protease (Fig. 1). To determine whether the Y354H polymorphism in T3A $\sigma 3$ confers resistance to protease inhibitors, T3A, T3D, and T3D- $\sigma 3$ Y354H were tested for the capacity to replicate in the presence of protease inhibitor E64. L929 cells were incubated in medium supplemented to contain 100 or 200 μ M E64, adsorbed with T3A, T3D, and T3D- $\sigma 3$ Y354H, and incubated in the presence or absence of E64 for 24 h. Cells were lysed, and viral titers in cell lysates were determined by plaque assay (Fig. 2). Despite the presence of histidine at position 354 in T3A $\sigma 3$, yields of T3A were reduced 259-fold, approximating the reduction observed for T3D, 195-fold, in the presence of 100 μ M E64, whereas yields of T3D- $\sigma 3$ Y354H were diminished less than 10-fold at this E64 concentration. Replication of T3A and T3D was completely ablated in the presence of 200 μ M E64, but yields of T3D- $\sigma 3$ Y354H were not further diminished. These findings suggest that one or more of the additional polymorphisms displayed by T3A $\sigma 3$ suppresses the Y354H phenotype and restores optimal $\sigma 3$ stability.

G198E Confers Susceptibility to E64 in Context of Y354H—To identify residues in T3A $\sigma 3$ that suppress the capacity of the Y354H polymorphism to confer viral growth in the presence of protease inhibitors, we engineered a panel of reovirus variants that incorporate single T3A-T3D polymorphisms in the context of T3D- $\sigma 3$ Y354H but are otherwise isogenic with T3D (Table 2). Despite several attempts, we could not recover T3D- $\sigma 3$ A28T,Y354H. In addition, T3D- $\sigma 3$ S233L,Y354H was recovered only with a concomitant glycine-to-tryptophan mutation at position 198 of $\sigma 3$. Each of the other variants was rescued and propagated to high titer working stocks.

We tested each of the variant viruses for replication in the presence of E64 (Fig. 3). As before, yields of T3A and T3D were diminished substantially by this inhibitor, whereas yields of T3D- $\sigma 3$ Y354H were only modestly impaired. Similarly, yields of T3D- $\sigma 3$ E108A, T3D- $\sigma 3$ I180V, T3D- $\sigma 3$ S215N, and T3D- $\sigma 3$ I347T were only slightly diminished by E64. In sharp contrast, yields of T3D- $\sigma 3$ G198E,Y354H were markedly decreased in the presence of E64, approximating those of T3A and T3D. These findings suggest that a glycine-to-glutamic acid mutation at position 198 independently suppresses the Y354H phenotype in T3A and enhances its sensitivity to the protease inhibitor E64.

Cathepsin L Sensitivity of T3A-T3D Variant Viruses—Cathepsin proteases catalyze reovirus disassembly within cellular endosomes (16, 33). To determine whether T3A-T3D polymorphisms alter capsid disassembly when treated with endosomal proteases, virions of T3A, T3D, T3D- $\sigma 3$ Y354H, and the T3A-T3D variants were digested *in vitro* with purified human cathepsin L (34). At 30-min intervals, aliquots were removed from the digestion mixtures, and viral proteins were resolved by SDS-PAGE and visualized using colloidal blue staining (Fig.

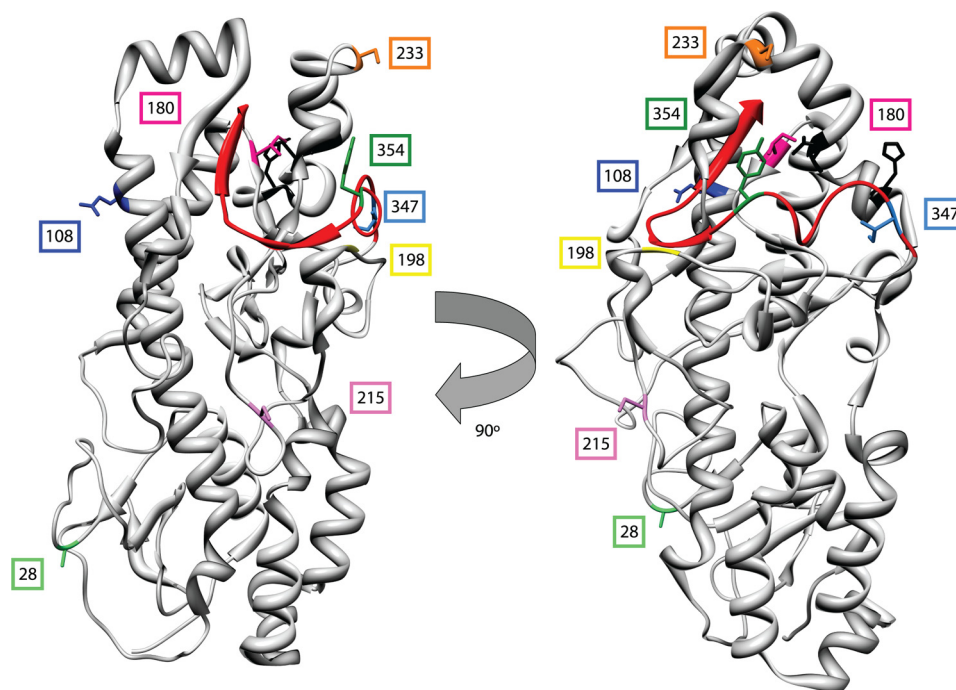


FIGURE 1. Location of polymorphic residues in strains T3A and T3D $\sigma 3$ proteins. A crystal structure of T3D $\sigma 3$ (21) is shown highlighting polymorphic residues in T3A and T3D $\sigma 3$ proteins, including Tyr-354 (dark green), which is altered in reovirus variants selected for enhanced disassembly kinetics (23, 24, 39). The virion-distal domain of $\sigma 3$ including the C terminus (depicted in red) is at the top of the figure. The virion-proximal region including the N terminus is at the bottom. Putative cathepsin L cleavage sites (determined for strain type 1 Lang) between amino acids 243 and 244 and between 250 and 251 are depicted in black (16).

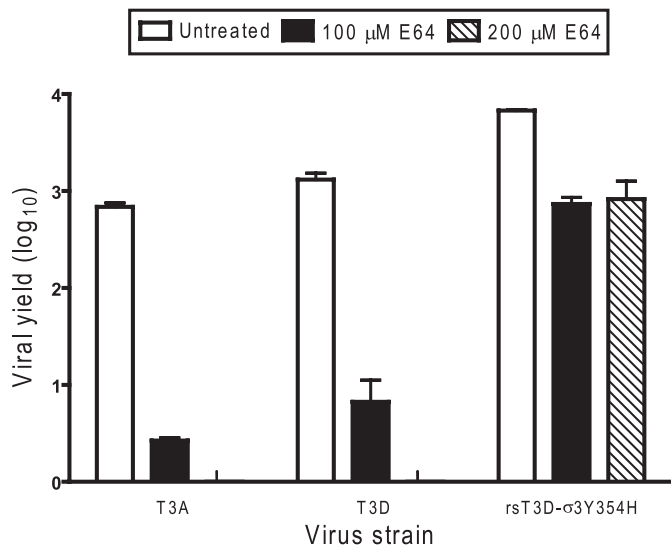


FIGURE 2. Replication of T3A, T3D, and rsT3D- $\sigma 3$ Y354H in L929 cells treated with E64. Monolayers of L929 cells were preincubated for 4 h in medium supplemented with or without E64 at the concentrations shown. The medium was removed, and cells were adsorbed with virus at an m.o.i. of 2 pfu/cell. After adsorption for 1 h, the inoculum was removed, and fresh medium with or without E64 was added. After incubation at 37 °C for 24 h, cells were frozen and thawed twice, and viral titers were determined by plaque assay. The results are presented as the mean viral yields, calculated by dividing titer at 24 h by titer at 0 h for each concentration of E64, for triplicate experiments. Yields of less than zero are not shown. Error bars indicate S.D.

4A). Intensity of the band corresponding to $\sigma 3$ remained relatively constant for T3A and T3D over the 240-min time course, as did the band corresponding to $\mu 1\text{C}$. However, in these experiments, T3D- $\sigma 3$ Y354H displayed almost complete loss of $\sigma 3$ protein within 60 min. In addition, the band corresponding to

TABLE 2

Reovirus variants in which polymorphic residues in T3D $\sigma 3$ are exchanged with those in T3A $\sigma 3$

Reovirus variants were engineered using plasmid-based reverse genetics. Each reovirus variant is isogenic with T3D with the exception of His-354 and a single additional T3A residue as shown. Bold and italics indicate viruses that were not successfully recovered.

Virus strain	Amino acid position							
	28	108	180	198	215	233	347	354
T3D	A	E	I	G	S	S	I	Y
T3A	T	A	V	E	N	L	T	H
T3D- $\sigma 3$ Y354H	A	E	I	G	S	S	I	H
<i>T3D-$\sigma 3$A28T,Y354H</i>	<i>T</i>	<i>E</i>	<i>I</i>	<i>G</i>	<i>S</i>	<i>S</i>	<i>I</i>	<i>H</i>
T3D- $\sigma 3$ E108A,Y354H	A	A	I	G	S	S	I	H
T3D- $\sigma 3$ I180V,Y354H	A	E	V	G	S	S	I	H
T3D- $\sigma 3$ G198E,Y354H	A	E	I	E	S	S	I	H
T3D- $\sigma 3$ S215N,Y354H	A	E	I	G	N	S	I	H
<i>T3D-$\sigma 3$S233L,Y354H</i>	<i>A</i>	<i>E</i>	<i>I</i>	<i>G</i>	<i>S</i>	<i>L</i>	<i>I</i>	<i>H</i>
T3D- $\sigma 3$ I347T,Y354H	A	E	I	G	S	S	T	H

$\mu 1\text{C}$ in T3D- $\sigma 3$ Y354H diminished in intensity over the course of protease treatment, and the appearance of a band corresponding to the δ fragment of $\mu 1\text{C}$ was noted for this virus. Each of the variant viruses was observed to undergo disassembly with kinetics similar to those of T3D- $\sigma 3$ Y354H (Fig. 4A) with the exception of T3D- $\sigma 3$ G198E,Y354H, which displayed a digestion profile similar to that of T3A and T3D.

We quantified the intensity of protein bands corresponding to $\sigma 3$ using an Odyssey infrared imaging system (Fig. 4B). To control for differences in gel loading, the band intensity of $\sigma 3$ protein was normalized to that of reovirus core protein $\sigma 2$, which is resistant to protease cleavage under these conditions. The $\sigma 3/\sigma 2$ ratio of T3A and T3D slightly decreased over the time course tested. The $\sigma 3/\sigma 2$ ratio of T3D- $\sigma 3$ Y354H and the variant viruses rapidly approached zero (Fig. 4B), with the nota-

ble exception of T3D- σ 3G198E,Y354H. For this virus, the σ 3/ σ 2 ratio approximated the T3D σ 3/ σ 2 ratio throughout the digestion time course. We conclude that G198E stabilizes σ 3 in the context of Y354H.

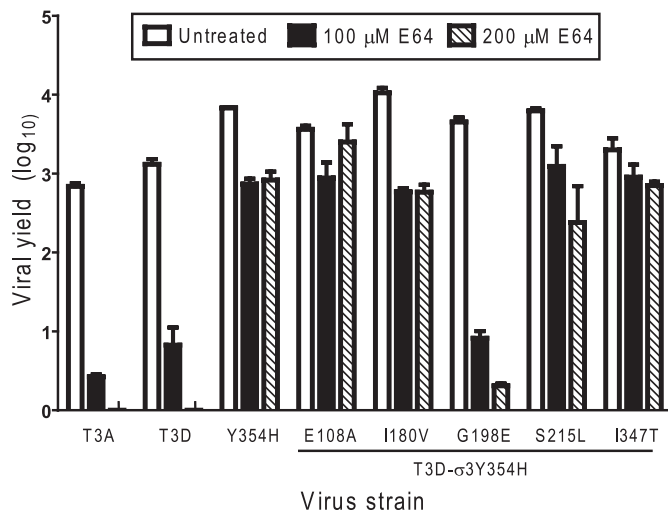


FIGURE 3. E64 susceptibility of T3A-T3D variant viruses. Monolayers of L929 cells were preincubated for 4 h in medium supplemented with or without E64 at the concentrations shown. The medium was removed, and cells were adsorbed with virus at an m.o.i. of 2 pfu/cell. After adsorption for 1 h, the inoculum was removed, and fresh medium with or without E64 was added. After incubation at 37 °C for 24 h, cells were frozen and thawed twice, and viral titers were determined by plaque assay. The results are presented as the mean viral yields, calculated by dividing titer at 24 h by titer at 0 h for each concentration of E64, for triplicate experiments. Yields of less than zero are not shown. Error bars indicate S.D.

Specific Infectivity of Reovirus Variants—We next considered the possibility that one or more of the σ 3 polymorphisms in our panel of variant reovirus strains might affect assembly of σ 3 onto nascent virions and thus compromise infectivity. To test this hypothesis, we examined the specific infectivity of our variant panel by calculating particle/pfu ratios for several independent preparations of each virus (Fig. 5). We observed that most of the virion stocks tested displayed particle/pfu ratios between 300 and 1000, consistent with reported values for type 3 reovirus strains (35) and our previous observations (data not shown). Although we observed some prep-to-prep variation, there were no significant differences between the variant and parental viruses (analysis of variance, $p > 0.05$). Therefore, the σ 3 mutations introduced in our variant panel do not substantially affect reovirus replicative efficiency and thus are not likely to alter capsid assembly.

Outer Capsid Mutations Affect Reovirus Heat Sensitivity—To assess whether the differences in protease sensitivity of our variant viruses correlate with biochemical measures of capsid stability, we determined the relative loss of titer of our variant panel following heat treatment. Samples of each virus were diluted to a titer of 2×10^8 and placed at 55 °C for 1 h. Aliquots were removed at 15-min intervals, and titers were determined by plaque assay (Fig. 6). We observed that T3D- σ 3Y354H lost titer significantly more rapidly (Student's t test, $p < 0.05$) at elevated temperature than did either T3A or T3D. Additionally, each of the variant viruses tested lost titer at rates similar to T3D- σ 3Y354H, again with the exception

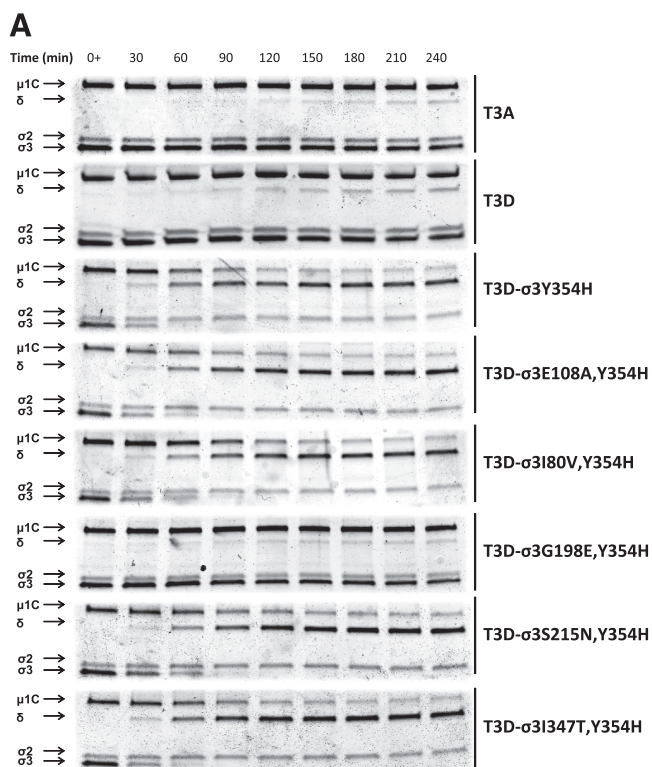
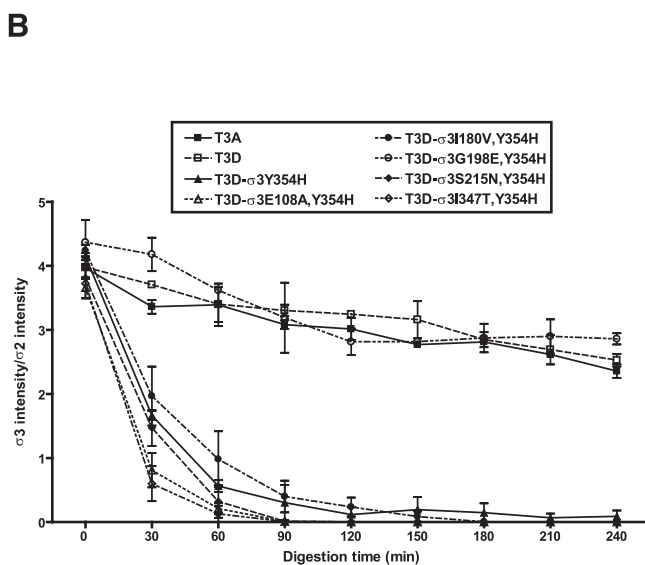


FIGURE 4. Digestion of reovirus strains with cathepsin L. A, purified virions were treated with human cathepsin L (34) for the intervals shown and loaded into wells of 4–20% gradient polyacrylamide gels. After electrophoresis, the gels were stained with colloidal blue (Invitrogen). Viral proteins μ 1C, δ , σ 2, and σ 3 are labeled at the left. The experiments shown are representative of two performed for each virus. B, intensities of bands corresponding to reovirus proteins were quantified using the Odyssey software package (LI-COR). Results are expressed as the ratio of σ 3 band intensity to σ 2 band intensity to control for differences in loading for two independent experiments. Error bars indicate S.D.



Determinants of Reovirus Outer Capsid Disassembly

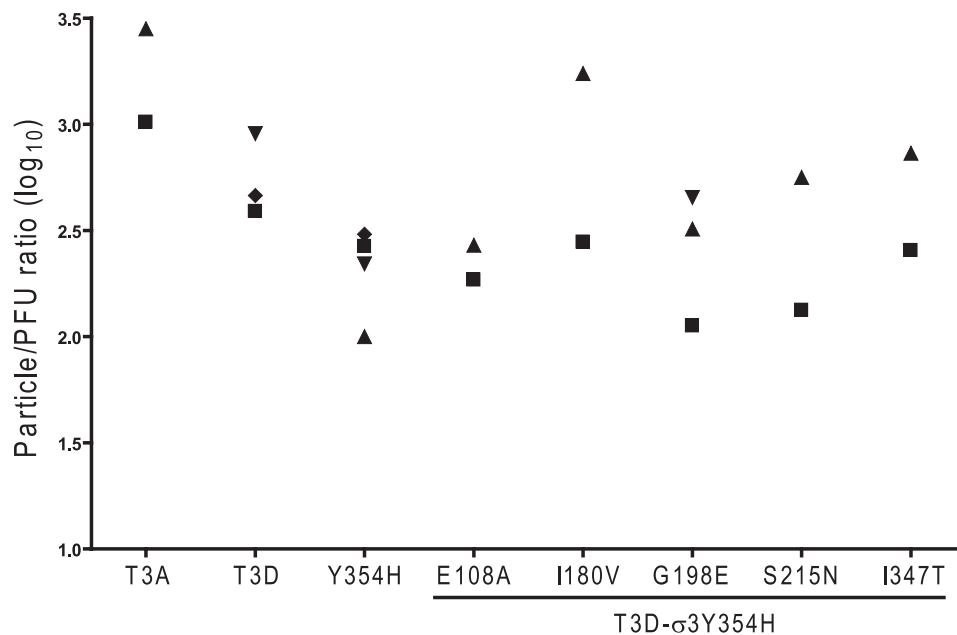


FIGURE 5. **Infectivity of reovirus variants.** Purified virions of variant viruses were generated from independent cultures of L929 cells ($\sim 4 \times 10^8$ cells) using CsCl gradient centrifugation. Particle number was quantified using the equivalence of $1 A_{260} = 2.1 \times 10^{12}$ particles/ml. The titer of each preparation was determined by plaque assay. The results are presented as particle/pfu ratio. Data points indicate independent viral purifications.

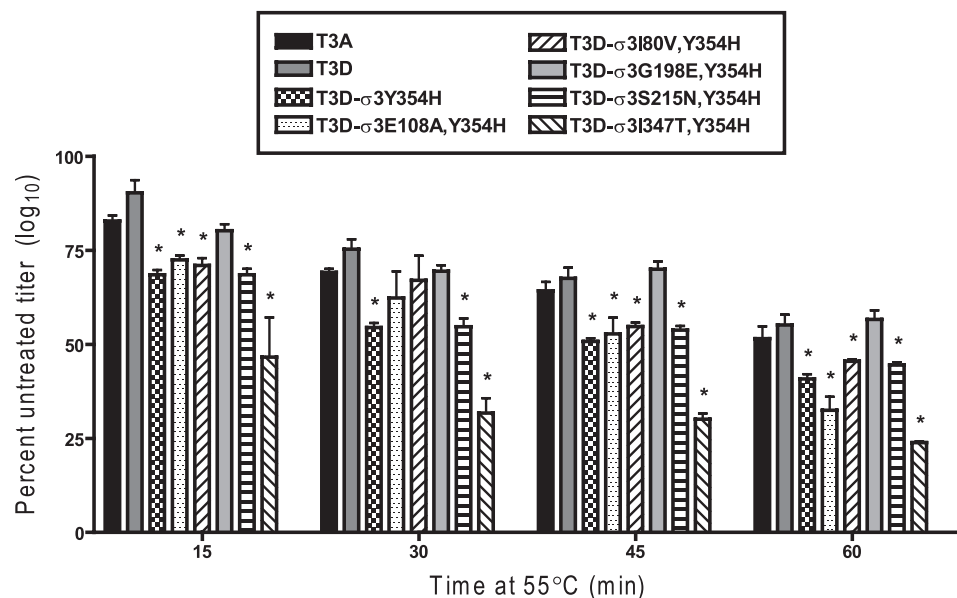


FIGURE 6. **Resistance of reovirus variants to inactivation by heat.** Purified virions of reovirus variants were diluted to a concentration of 2×10^8 particles/ml in virion storage buffer and incubated at 55°C for 60 min. At 15-min intervals, samples were removed and placed on ice for 15 min. Titers were determined by plaque assay. Results are presented as the percentage of mean viral titer of untreated samples per interval of incubation, for triplicate experiments. Error bars indicate S.D.; *, $p \leq 0.05$ in comparison with T3D.

of T3D- σ 3G198E,Y354H. The rate of titer loss for that virus did not significantly differ from T3D. The fact that enhanced protease sensitivity and altered sensitivity to heat are correlated in the context of Y354H suggests that this residue controls both properties through a common structural mechanism.

Enhanced Outer Capsid Protease Sensitivity Facilitates Endosomal Escape—Following binding to cell-surface receptors, reovirus particles are thought to be internalized via clathrin-dependent endocytosis (10–12, 36). Cleavage of σ 3 by endosomal cathepsins is required for particle disassembly and

subsequent escape from the endosome into the cytoplasm (14–19, 37). To determine whether the enhanced susceptibility to proteolytic cleavage mediated by σ 3-Y354H alters the kinetics with which reovirus particles escape host cell endosomes, we took advantage of the fact that reovirus disassembly is abrogated by preventing the pH drop required for efficient cathepsin cleavage when intact particles are still resident in endosomes (7, 38). We adsorbed monolayers of L929 cells with variant reovirus strains at 4°C for 1 h to synchronize viral attachment, warmed the cells to 37°C , and added ammonium chloride at various intervals following

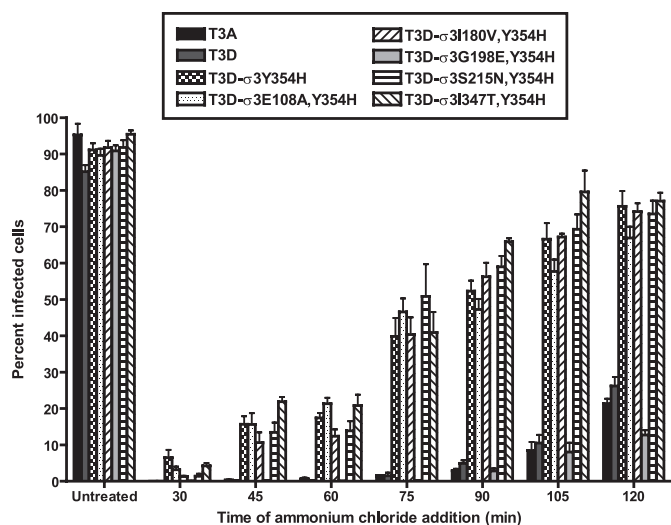


FIGURE 7. Kinetics of ammonium chloride bypass by reovirus variants. Monolayers of L929 cells were adsorbed with reovirus variants at an m.o.i. of 25 pfu/cell at 4 °C. After adsorption for 1 h, the inoculum was removed, fresh prewarmed medium was added, and cells were warmed to 37 °C. At the times shown after adsorption, ammonium chloride was added to a final concentration of 25 mM. After incubation at 37 °C for 20 h, cells were fixed with methanol at -20 °C, and infectivity was assessed by indirect immunofluorescence. The results are presented as the percentage of cells infected, normalized to untreated wells, for triplicate experiments. Error bars indicate S.D.

warming to prevent endosome acidification. Cells were incubated overnight and scored for viral infectivity by indirect immunofluorescence (Fig. 7). Variant viruses containing the $\sigma 3$ -Y354H mutation, with the exception of T3D- $\sigma 3$ G198E,Y354H, escaped ammonium chloride blockade as much as 60 min earlier than either T3A or T3D. These findings indicate that enhanced outer capsid protease sensitivity accelerates access of reovirus to the cytoplasm for subsequent steps in its replication cycle.

Residue 198 Second-site Changes—One of the variant viruses, T3D- $\sigma 3$ S233L,Y354H, could be recovered only in combination with a glycine-to-tryptophan substitution at position 198. In addition, multiple isolates of T3D- $\sigma 3$ I347T,Y354H contained *de novo* glycine-to-valine mutations at position 198. To determine whether these second-site mutations affect reovirus disassembly, we tested the effect of E64 treatment on the replication of variants containing these alterations (Fig. 8). Viruses containing either Val-198 or Trp-198 in the context of Y354H had modestly enhanced E64 sensitivity in comparison with that of T3D- $\sigma 3$ Y354H. In particular, introduction of Val-198 restored the E64 sensitivity of T3D- $\sigma 3$ G198V,I347T,Y354H to that of T3D. The E64 sensitivity of T3D- $\sigma 3$ G198W,S233L,Y354H was intermediate between that of T3D and T3D- $\sigma 3$ Y354H, although T3D- $\sigma 3$ G198W,S233L,Y354H produced lower peak titers in the absence of protease inhibitor than did T3D. These findings underscore the importance of residue 198 in determining $\sigma 3$ stability and suggest that the molecular basis of Y354H suppression may differ depending on the biochemical nature of the amino acid at that position.

DISCUSSION

Nonenveloped viruses must undergo particle disassembly to initiate an infectious cycle. The rate-limiting step in reovirus

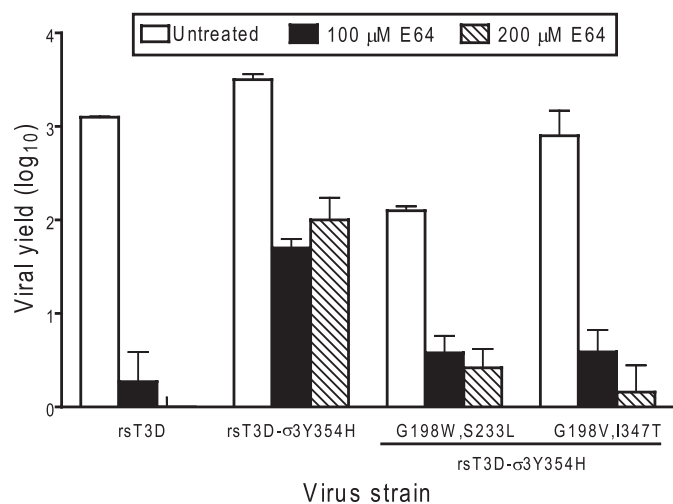


FIGURE 8. E64 sensitivity of reovirus strains with second-site mutations. Monolayers of L929 cells were preincubated for 4 h in medium supplemented with or without E64 at the concentrations shown. The medium was removed, and cells were adsorbed with reovirus strains at an m.o.i. of 2 pfu/cell. After adsorption for 1 h, the inoculum was removed, and fresh medium with or without E64 was added. After incubation at 37 °C for 24 h, cells were frozen and thawed twice, and viral titers were determined by plaque assay. The results are presented as the mean viral yields, calculated by dividing titer at 24 h by titer at 0 h for each concentration of E64, for triplicate experiments. Yields of less than zero are not shown. Error bars indicate S.D.

disassembly is the enzyme-mediated cleavage of $\sigma 3$ protein in endosomes of infected cells (7, 11, 14, 17, 18). Surface features of $\sigma 3$ that influence its capacity to serve as an enzyme substrate are not well understood. A single mutation in reovirus T3D $\sigma 3$ protein, Y354H, enhances susceptibility of the reovirus virion to protease and confers viral resistance to protease inhibitors (14, 22, 24, 39). Structural evidence suggests that enhanced susceptibility to protease conferred by Y354H is due to an intramolecular rearrangement of domains in $\sigma 3$ that enhances access to internal protease cleavage sites (22). However, this model has not been explicitly tested. Selection of reovirus mutants under conditions that diminish endosomal protease activity yields viruses containing the $\sigma 3$ -Y354H mutation (14, 24, 39), suggesting that capsid-destabilizing mutations are advantageous in certain settings. The importance of capsid stability in other phases of the reovirus life cycle is unclear.

In this study, we identified a new surface determinant of reovirus capsid stability located at position 198 in $\sigma 3$. To our knowledge, reovirus strain T3A is the only field isolate strain reported to date that contains a histidine at position 354 (25). Based on our previous understanding of the phenotype of virus strains containing $\sigma 3$ -Y354H, we anticipated that T3A would be resistant to protease inhibitors and display enhanced susceptibility to proteases in comparison with T3D. Surprisingly, we found that T3A has E64 sensitivity similar to that of T3D despite the presence of His-354 in $\sigma 3$. We also observed that T3A and T3D have similar *in vitro* disassembly kinetics when treated with the endosomal protease cathepsin L. Based on these observations, we hypothesized that other residues in T3A $\sigma 3$ that differ from T3D $\sigma 3$ suppress the Y354H phenotype.

We used plasmid-based reverse genetics to generate a panel of reovirus variants to test the contributions made by each T3A-T3D polymorphic residue to capsid stability in an other-

Determinants of Reovirus Outer Capsid Disassembly

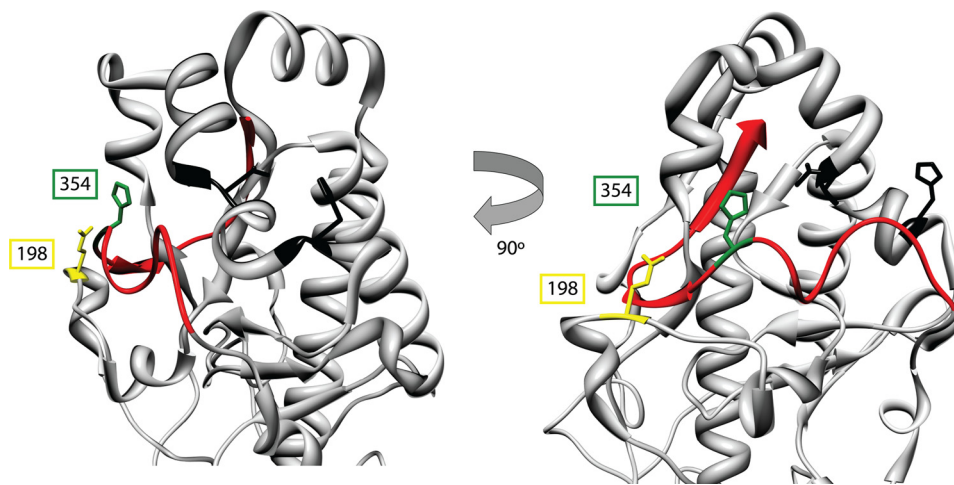


FIGURE 9. **Residues 198 and 354 define an amino acid network regulating $\sigma 3$ proteolysis.** The virion-distal domain of T3D $\sigma 3$ is shown. The C terminus is depicted in red. Glu-198 and His-354 are modeled in yellow and green, respectively, and are drawn in stick representation. The amino acids corresponding to the two putative cathepsin L cleavage sites, residues Val-243-Thr-244 and Gly-250-His251 (16), are shown in black in stick representation.

wise isogenic background that includes Y354H. Despite numerous attempts, a virus containing an aspartate-to-threonine change at position 28, T3D- $\sigma 3$ D28T,Y354H, could not be recovered. Amino acid 28 is located in a virion-proximal domain of $\sigma 3$ (Fig. 1) that is important for interactions of $\sigma 3$ with $\mu 1$ during virion assembly (40). It is possible that mutations at position 28 impair interactions between $\sigma 3$ and $\mu 1$ (40), hindering recovery of T3D- $\sigma 3$ D28T,Y354H. The recovered variant viruses had no overt defects in replication or specific infectivity (Fig. 5). All of the T3A-T3D variant viruses are resistant to cysteine protease inhibitor E64 and thus phenocopy T3D- $\sigma 3$ Y354H, except the virus containing a glycine-to-glutamate change at position 198, T3D- $\sigma 3$ G198E,Y354H. Yields of T3D- $\sigma 3$ G198E,Y354H are markedly diminished in cells treated with E64. Concordantly, all members of the T3A-T3D variant panel except T3D- $\sigma 3$ G198E,Y354H display kinetics of digestion by cathepsin L similar to T3D- $\sigma 3$ Y354H. Moreover, we also observed that all of the variant viruses escape an endosomal infectivity block more rapidly than T3A or T3D, again excepting T3D- $\sigma 3$ G198E,Y354H. Together, these results provide strong evidence that suppression of the Y354H phenotype in T3A is solely attributable to the glycine-to-glutamate polymorphism at position 198.

Another virus, T3D- $\sigma 3$ S233L,Y354H, could be recovered only with an accompanying glycine-to-tryptophan mutation at position 198. In addition, four of the seven T3D- $\sigma 3$ I347T,Y354H clones sequenced contained a second-site mutation at position 198, specifically, a glycine-to-valine substitution. We found that T3D- $\sigma 3$ G198W,S233L,Y354H and T3D- $\sigma 3$ G198V,I347T,Y354H had increased E64 susceptibility in comparison with that of T3D- $\sigma 3$ Y354H, although neither virus was as sensitive to this protease inhibitor as was T3A or T3D. The observation of two different, independently arising mutations at position 198 in $\sigma 3$ supports the conclusion that residue 198 is a key determinant of $\sigma 3$ protease susceptibility. It is plausible that mutations at positions 233 and 347 enhance the selection of Y354H-suppressive mutations, perhaps by further destabilizing $\sigma 3$.

The $\sigma 3$ C terminus is thought to control the rate of $\sigma 3$ cleavage by restricting protease access to cleavage sites located internally within the protein (16, 22, 40). The C-terminal domain of $\sigma 3$ localizes to a solvent-exposed surface of the $\sigma 3/\mu 1$ heterohexamer and is not predicted to directly interact with other viral proteins (40). There is some structural evidence suggesting that the Y354H mutation accelerates $\sigma 3$ cleavage by dislocating the $\sigma 3$ C terminus, affording easier access to internal cleavage sites (22). The observation that residue 198 suppresses Y354H indirectly supports this model (Fig. 9). The $\sigma 3$ C terminus (red) overlies the putative cathepsin L cleavage sites (black), located between residues 243–244 and 250–251. Substitution of Tyr-354 in the C terminus (green) with histidine, a basic amino acid, may disrupt hydrophobic interactions required for proper folding of the $\sigma 3$ C terminus. Low resolution cryo-EM reconstructions of $\sigma 3$ -Y354H reveal added density in a hinge region between the virion-proximal and virion-distal $\sigma 3$ lobes that is absent in T3D $\sigma 3$ (22). This increase in density may represent the dislocated C terminus of the molecule. Residue 198 in $\sigma 3$ is located on a loop directly opposed to residue 354. It is possible that the glycine-to-glutamate polymorphism observed in T3A stabilizes the C terminus through charge-charge interactions with His-354. Substitution of residue 198 with hydrophobic amino acids, such as tryptophan and valine as observed in this study, may also stabilize the $\sigma 3$ C terminus, perhaps by steric interactions that limit its mobility. Our finding that alterations at positions 233 and 347 elicit compensatory hydrophobic mutations at position 198 suggests that more complex intramolecular rearrangements of $\sigma 3$ may occur in those viruses. Interestingly, a virus selected for growth in the presence of E64, D-EA3, contains two mutations in $\sigma 3$, the expected Y354H and a glycine-to-arginine change at position 198 (39). In that study, Arg-198 failed to suppress Y354H, perhaps because it fails to neutralize the basic charge of His-354. Although our results suggest that $\sigma 3$ residue 198 is a key surface determinant of reovirus outer capsid stability, the ready selection of mutations at position 198 that incorporate amino acids with a range of biochemical properties may point to subtle roles

for residue 198 either in maintaining capsid stability or in other aspects of reovirus replication.

The observation that $\sigma 3$ -Y354H is rare in circulating reovirus strains and exists coincident with suppressor mutations in T3A $\sigma 3$ suggests that reovirus strains suffer a fitness penalty for mutations that destabilize the outer capsid. The reovirus life cycle involves fecal-oral transmission between infected hosts, a step that requires some degree of resistance to degradation. Viruses with diminished outer capsid stability may have decreased viability outside a mammalian host, which would reduce their likelihood of encountering a new host. We note that viruses containing uncompensated $\sigma 3$ -Y354H lose titer more rapidly at elevated temperature than T3A or T3D (Fig. 6), suggesting that such viruses may have diminished environmental persistence or decreased infectivity from fomite surfaces. However, it is possible that destabilization of the outer capsid adversely affects other aspects of viral replication or virus-host interactions. The optimum stability of reovirus capsid structures may also depend on the specific proteolytic milieu of the various physiological compartments encountered by viral particles during the course of infection. More work is necessary to define the precise constraints on reovirus capsid stability throughout the viral life cycle. The findings reported in this study identify a network of residues that determine the stability of reovirus $\sigma 3$ and provide insight into mechanisms used by nonenveloped viruses to maintain optimum capsid stability.

Acknowledgments—We express our appreciation to Karl Boehme and Greg Wilson for careful review of the manuscript and to Chris Aiken for helpful suggestions. We thank John Mort for the kind gift of purified cathepsin L. Additional support was provided by United States Public Health Service Awards CA68485 for the Vanderbilt Cancer Center and DK20593 for the Vanderbilt Diabetes Research and Training Center.

REFERENCES

- Wilson, I. A., Skehel, J. J., and Wiley, D. C. (1981) Structure of the hemagglutinin membrane glycoprotein of influenza virus at 3 Å resolution. *Nature* **289**, 366–373
- Skehel, J. J., Bayley, P. M., Brown, E. B., Martin, S. R., Waterfield, M. D., White, J. M., Wilson, I. A., and Wiley, D. C. (1982) Changes in the conformation of influenza virus hemagglutinin at the pH optimum of virus-mediated membrane fusion. *Proc. Natl. Acad. Sci. U.S.A.* **79**, 968–972
- Baker, K. A., Dutch, R. E., Lamb, R. A., and Jardetzky, T. S. (1999) Structural basis for paramyxovirus-mediated membrane fusion. *Mol. Cell* **3**, 309–319
- Chan, D. C., Fass, D., Berger, J. M., and Kim, P. S. (1997) Core structure of gp41 from the HIV envelope glycoprotein. *Cell* **89**, 263–273
- Weissenhorn, W., Dessen, A., Harrison, S. C., Skehel, J. J., and Wiley, D. C. (1997) Atomic structure of the ectodomain from HIV-1 gp41. *Nature* **387**, 426–430
- Wiethoff, C. M., Wodrich, H., Gerace, L., and Nemerow, G. R. (2005) Adenovirus protein VI mediates membrane disruption following capsid disassembly. *J. Virol.* **79**, 1992–2000
- Sturzenbecker, L. J., Nibert, M., Furlong, D., and Fields, B. N. (1987) Intracellular digestion of reovirus particles requires a low pH and is an essential step in the viral infectious cycle. *J. Virol.* **61**, 2351–2361
- Dryden, K. A., Wang, G., Yeager, M., Nibert, M. L., Coombs, K. M., Furlong, D. B., Fields, B. N., and Baker, T. S. (1993) Early steps in reovirus infection are associated with dramatic changes in supramolecular structure and protein conformation: analysis of virions and subviral particles by cryo-electron microscopy and image reconstruction. *J. Cell Biol.* **122**, 1023–1041
- Schiff, L. A., Nibert, M. L., and Tyler, K. L. (2007) in *Fields Virology* (Knipe, D. M., and Howley, P. M., eds), Fifth Ed., pp. 1853–1915, Lippincott Williams & Wilkins, Philadelphia
- Borsa, J., Morash, B. D., Sargent, M. D., Copps, T. P., Lievaart, P. A., and Szekely, J. G. (1979) Two modes of entry of reovirus particles into L cells. *J. Gen. Virol.* **45**, 161–170
- Borsa, J., Sargent, M. D., Lievaart, P. A., and Copps, T. P. (1981) Reovirus: evidence for a second step in the intracellular uncoating and transcriptase activation process. *Virology* **111**, 191–200
- Ehrlich, M., Boll, W., Van Oijen, A., Hariharan, R., Chandran, K., Nibert, M. L., and Kirchhausen, T. (2004) Endocytosis by random initiation and stabilization of clathrin-coated pits. *Cell* **118**, 591–605
- Maginnis, M. S., Forrest, J. C., Kopecky-Bromberg, S. A., Dickeson, S. K., Santoro, S. A., Zutter, M. M., Nemerow, G. R., Bergelson, J. M., and Dermody, T. S. (2006) $\beta 1$ integrin mediates internalization of mammalian reovirus. *J. Virol.* **80**, 2760–2770
- Baer, G. S., and Dermody, T. S. (1997) Mutations in reovirus outer capsid protein $\sigma 3$ selected during persistent infections of L cells confer resistance to protease inhibitor E64. *J. Virol.* **71**, 4921–4928
- Baer, G. S., Ebert, D. H., Chung, C. J., Erickson, A. H., and Dermody, T. S. (1999) Mutant cells selected during persistent reovirus infection do not express mature cathepsin L and do not support reovirus disassembly. *J. Virol.* **73**, 9532–9543
- Ebert, D. H., Deussing, J., Peters, C., and Dermody, T. S. (2002) Cathepsin L and cathepsin B mediate reovirus disassembly in murine fibroblast cells. *J. Biol. Chem.* **277**, 24609–24617
- Chang, C. T., and Zweerink, H. J. (1971) Fate of parental reovirus in infected cell. *Virology* **46**, 544–555
- Silverstein, S. C., Astell, C., Levin, D. H., Schonberg, M., and Acs, G. (1972) The mechanisms of reovirus uncoating and gene activation *in vivo*. *Virology* **47**, 797–806
- Ivanovic, T., Agosto, M. A., Zhang, L., Chandran, K., Harrison, S. C., and Nibert, M. L. (2008) Peptides released from reovirus outer capsid form membrane pores that recruit virus particles. *EMBO J.* **27**, 1289–1298
- Ebert, D. H., Kopecky-Bromberg, S. A., and Dermody, T. S. (2004) Cathepsin B is inhibited in mutant cells selected during persistent reovirus infection. *J. Biol. Chem.* **279**, 3837–3851
- Olland, A. M., Jané-Valbuena, J., Schiff, L. A., Nibert, M. L., and Harrison, S. C. (2001) Structure of the reovirus outer capsid and dsRNA-binding protein $\sigma 3$ at 1.8 Å resolution. *EMBO J.* **20**, 979–989
- Wilson, G. J., Nason, E. L., Hardy, C. S., Ebert, D. H., Wetzel, J. D., Venkataram Prasad, B. V., and Dermody, T. S. (2002) A single mutation in the carboxyl terminus of reovirus outer capsid protein $\sigma 3$ confers enhanced kinetics of $\sigma 3$ proteolysis, resistance to inhibitors of viral disassembly, and alterations in $\sigma 3$ structure. *J. Virol.* **76**, 9832–9843
- Wetzel, J. D., Wilson, G. J., Baer, G. S., Dunnigan, L. R., Wright, J. P., Tang, D. S., and Dermody, T. S. (1997) Reovirus variants selected during persistent infections of L cells contain mutations in the viral S1 and S4 genes and are altered in viral disassembly. *J. Virol.* **71**, 1362–1369
- Clark, K. M., Wetzel, J. D., Gu, Y., Ebert, D. H., McAbee, S. A., Stoneman, E. K., Baer, G. S., Zhu, Y., Wilson, G. J., Prasad, B. V., and Dermody, T. S. (2006) Reovirus variants selected for resistance to ammonium chloride have mutations in viral outer capsid protein $\sigma 3$. *J. Virol.* **80**, 671–681
- Kedl, R., Schmechel, S., and Schiff, L. (1995) Comparative sequence analysis of the reovirus S4 genes from 13 serotype 1 and serotype 3 field isolates. *J. Virol.* **69**, 552–559
- Rosen, L., Hovis, J. F., Mastrotta, F. M., Bell, J. A., and Huebner, R. J. (1960) Observations on a newly recognized virus (Abney) of the reovirus family. *American Journal of Hygiene* **71**, 258–265
- Kobayashi, T., Ooms, L. S., Ikizler, M., Chappell, J. D., and Dermody, T. S. (2010) An improved reverse genetics system for mammalian orthoreoviruses. *Virology* **398**, 194–200
- Kobayashi, T., Antar, A. A., Boehme, K. W., Danthi, P., Eby, E. A., Guglielmi, K. M., Holm, G. H., Johnson, E. M., Maginnis, M. S., Naik, S., Skelton, W. B., Wetzel, J. D., Wilson, G. J., Chappell, J. D., and Dermody, T. S. (2007) A plasmid-based reverse genetics system for animal double-

Determinants of Reovirus Outer Capsid Disassembly

- stranded RNA viruses. *Cell Host Microbe*. **1**, 147–157
29. Virgin, H. W., 4th, Bassel-Duby, R., Fields, B. N., and Tyler, K. L. (1988) Antibody protects against lethal infection with the neurally spreading reovirus type 3 (Dearing). *J. Virol.* **62**, 4594–4604
 30. Furlong, D. B., Nibert, M. L., and Fields, B. N. (1988) $\sigma 1$ protein of mammalian reoviruses extends from the surfaces of viral particles. *J. Virol.* **62**, 246–256
 31. Laemmli, U. K. (1970) Cleavage of structural proteins during the assembly of the head of bacteriophage T4. *Nature* **227**, 680–685
 32. Smith, R. E., Zweerink, H. J., and Joklik, W. K. (1969) Polypeptide components of virions, top component, and cores of reovirus type 3. *Virology* **39**, 791–810
 33. Johnson, E. M., Doyle, J. D., Wetzel, J. D., McClung, R. P., Katunuma, N., Chappell, J. D., Washington, M. K., and Dermody, T. S. (2009) Genetic and pharmacologic alteration of cathepsin expression influences reovirus pathogenesis. *J. Virol.* **83**, 9630–9640
 34. Carmona, E., Dufour, E., Plouffe, C., Takebe, S., Mason, P., Mort, J. S., and Ménard, R. (1996) Potency and selectivity of the cathepsin L propeptide as an inhibitor of cysteine proteases. *Biochemistry* **35**, 8149–8157
 35. Hand, R., and Tamm, I. (1973) Reovirus: effect of noninfective viral components on cellular deoxyribonucleic acid synthesis. *J. Virol.* **11**, 223–231
 36. Maginnis, M. S., Mainou, B. A., Derdowski, A., Johnson, E. M., Zent, R., and Dermody, T. S. (2008) NPXY motifs in the $\beta 1$ integrin cytoplasmic tail are required for functional reovirus entry. *J. Virol.* **82**, 3181–3191
 37. Chandran, K., Farsetta, D. L., and Nibert, M. L. (2002) Strategy for nonenveloped virus entry: a hydrophobic conformer of the reovirus membrane penetration protein $\mu 1$ mediates membrane disruption. *J. Virol.* **76**, 9920–9933
 38. Dermody, T. S., Nibert, M. L., Wetzel, J. D., Tong, X., and Fields, B. N. (1993) Cells and viruses with mutations affecting viral entry are selected during persistent infections of L cells with mammalian reoviruses. *J. Virol.* **67**, 2055–2063
 39. Ebert, D. H., Wetzel, J. D., Brumbaugh, D. E., Chance, S. R., Stobie, L. E., Baer, G. S., and Dermody, T. S. (2001) Adaptation of reovirus to growth in the presence of protease inhibitor E64 segregates with a mutation in the carboxyl terminus of viral outer capsid protein $\sigma 3$. *J. Virol.* **75**, 3197–3206
 40. Liemann, S., Chandran, K., Baker, T. S., Nibert, M. L., and Harrison, S. C. (2002) Structure of the reovirus membrane penetration protein, $\mu 1$, in a complex with its protector protein, $\sigma 3$. *Cell* **108**, 283–295